Polymer Chemistry

TBD
poly-addition
trans-esterification
anionic ROP

1 bio-based diacid + x diepoxide → tunable epoxy vitrimers

Themed collection: Covalent Adaptable Networks

ROYAL SOCIETY
OF CHEMISTRY

PAPER
François Tournilhac, Matthieu Gresil *et al.*
Dicarboxylic acid-epoxy vitrimers: influence of the
off-stoichiometric acid content on cure reactions and
thermo-mechanical properties

Dicarboxylic acid-epoxy vitrimers: influence of the off-stoichiometric acid content on cure reactions and thermo-mechanical properties†

Quentin-Arthur Poutrel, [ID] [a,b] Jonny J. Blaker, [ID] [a] Constantinos Soutis, [ID] [b] François Tournilhac [ID] *[c] and Matthieu Gresil [ID] *[d]

The present study explores a broad range of stoichiometry, with the [epoxy]/[acyl] ratio ranging from excess to unity for commercial diepoxide/sebacic acid vitrimer formulations, with 1,5,7-triazabicyclo [4.4.0]dec-5-ene (TBD) used as the catalyst. In particular, it investigates to what extent side reactions promoted by off-stoichiometry mixtures can help achieve desirable thermomechanical properties (*i.e.* glass transition T_α, Young's modulus, strain at break, and strength) for an optimised vitrimer that behaves like a stiff material at room temperature, retaining its capacity to flow at high temperature while remaining insoluble. The possible role of TBD as an anionic initiator is tested in the homopolymerisation of epoxy and compared to a known anionic initiator, 2-phenylimidazole (2-PI). Attenuated total reflection infrared (ATR-IR) spectroscopy reveals different reaction speeds, but an identical scenario for either 2-PI or TBD. The acid + epoxy addition occurs first, then epoxy homopolymerisation takes place after di-carboxylic acid consumption; an ester typically forms in less than 20 min at 125 °C with TBD, while the formation of ether takes several hours. For all [epoxy]/[acyl] ratios ranging from 1:1 to 1:0.3, it is found that the integrity of the network is retained when subjected to 1,2,4 trichlorobenzene (TCB) solvent treatment. From the 1:1 to 1:0.75 epoxy to acyl ratio, the material retains full ability to flow and relax stresses under thermal stimulation, showing a 10 fold increase in viscosity and unchanged activation energy of about 100 kJ mol^{-1}. Beyond 1:0.6 stoichiometry, a gradual transition from vitrimer to non-exchangeable cross-linked materials is observed as these networks show only partial stress relaxation due to interpenetration in the polyether network.

Background

Polymer networks with reversible covalent links have been investigated as systems that are capable of topology rearrangement in response to excitation[1,2] (thermal or photochemical activation), as reviewed in the last 6 years.[3,4] Systems where reversibility involves chemical reactions occurring through a dissociative mechanism such as the Diels–Alder reaction[5] were first studied due to the wide range of

chemical reactions available.[6,7] In these systems, the dissociative mechanism means that whenever topology rearrangement is desired, existing links have to be broken before new links can be established, leading to a temporary drop in viscosity and loss of structural integrity once bond reversibility is activated. In contrast, a different family of reversible covalent networks can be envisioned where the formation of new bonds takes place before existing ones are broken, thus maintaining the integrity of the network throughout the exchange process. In 2005, Bowman and coworkers[8] described photo-induced plasticity in crosslinked polymers based on reversible chain-transfer reactions involving an associative mechanism, and, in 2011, Leibler and coworkers[9] introduced the concept of vitrimers – a class of polymer networks with dynamic links and/or crosslinks that became the example of associative exchange reactions upon thermal excitation. Vitrimers are insoluble thermoset-like polymers. Under thermal stimulation, bond exchanges are rapid, especially in the presence of a well-chosen catalyst. Thereby, the material can flow through reorganisation of the network

[a] Bio-Active Materials Group, Department of Materials, The University of Manchester, Manchester, UK

[b] Aerospace Research Institute, The University of Manchester, Manchester, UK

[c] Molecular, Macromolecular Chemistry, and Materials, ESPCI Paris, PSL University, CNRS, 10 rue Vauquelin, 75005 Paris, France. E-mail: francois.tournilhac@espci.fr

[d] i-Composites Lab, Department of Materials Science and Engineering, Monash University, Clayton, Australia. E-mail: matthieu.gresil@monash.edu

†Electronic supplementary information (ESI) available: Manufacture of vitrimer networks, IR analysis method, dynamic mechanical analysis, mechanical results, stress relaxation results, and creep results for all samples. See DOI: 10.1039/d0py00342e

topology; thus they have been proven to be heat-processable, recyclable and weldable, akin to thermoplastics.[10–12]

The present concept (*i.e.* covalent bond exchange) is not linked to any particular chemistry. In vitrimer prototypes, the possibility of building dynamic polyhydroxyl ester networks by thermoset chemistry has been demonstrated.[9] Since then, numerous examples of vitrimers based on various skeletons and involving a wide choice of exchange reactions, with and without catalysts, have been described.[13–22] Nonetheless, the epoxy chemistry used in the initial vitrimers remains appealing since it is based on the choice of industrially relevant monomers. Epoxy resins are heavily used in transport-, health-, electronic-, and energy-related technologies. Currently, a wide range of epoxy monomers and hardeners are commercially available or at least well described in the literature,[23,24] and virtually any combination of each is possible. Epoxy curing is an ensemble of ring-opening reactions with the ability to operate without solvent, without by-products – not even a molecule of water – and with low shrinkage.[25,26] Esterification and transesterification are among the most common reactions of organic chemistry, used on a large scale to produce[27] (and recycle) polyesters[28] and, more recently, in bio-diesel production,[29] for which vast literature on reaction conditions and catalysts is available.[30–34]

Epoxy based vitrimers are relatively new material systems that can be employed as matrix in fibre reinforced composite materials.[35,36] However, so far, the glass transition – an intrinsic property of thermosets, designated as T_g (measured by DSC) or T_α (measured by DMA) – has remained difficult to predict by any method other than trial and error. Often efforts made to increase the T_g (or T_α) above a certain value (depending on network compounds and curing conditions) lead to issues with the entire formulation in terms of compatibility, processing, degassing, and curing cycles.[37]

Epoxy–carboxylic acid vitrimer formulations reported in the literature to date[9,38–40] have mostly used a 1 : 1 epoxy to acyl ratio. The addition of one –COOH group to the epoxy ring generates one hydroxide for each ester formed, resulting in an equal concentration of both reactants for further exchanges by transesterification. Decreasing the epoxy to acyl ratio to 1 : 2 has been reported for some epoxy–anhydride formulations, and in all cases a decrease in weldability was observed.[10,35] The present work explores the effect of varying the stoichiometric ratio in the opposite direction, *i.e.* towards increasing the epoxy to acyl content. Altuna *et al.*[41,42] have shown that decreasing the acid content could lead to the formation of ethers through anionic homopolymerisation of the remaining epoxy as suggested by Matějka *et al.*[43] in the early 80s. Torkelson and coworkers[44] synthesised vitrimers containing a maximum of 40% fraction of permanent crosslinks to increase the creep resistance. Hoppe *et al.*[45] analysed the reaction of bisphenol-A diglycidyl ether, DGEBA with a stoichiometric amount of monocarboxylic acid and also with a variable excess of epoxy groups with a conventional tertiary amine as the catalyst. They obtained a gel when the ratio of epoxy to acid groups was higher than 3, but with a drop in the T_g from

90 to 0 °C. Recently, Altuna *et al.*[46] synthesised poly hydroxy-ester vitrimer networks with a fraction of non-exchangeable amine links as internal catalysts in the network; they developed a statistical analysis of the network structure to estimate the partition of the tertiary amine between sol and gel fractions.

Here, the effect of non-stoichiometry on vitrimer properties is investigated. In our experiments, epoxy vitrimer samples have been manufactured, using a commercial epoxy resin (mixture of diepoxide monomers) and sebacic acid (SA) as a hardener, with different stoichiometries (from 1 : 0.3 to 1 : 1 epoxy/acyl ratio), and 1,5,7-triazabicyclo[4.4.0]dec-5-ene (TBD) as the organic catalyst.

Materials and methods

Araldite LY 564 was chosen for its versatility as a low-viscosity resin for a variety of applications, including materials for electronics or structural composites. Sebacic acid is a classic bio-based molecule used as a monomer in polyamide chemistry and already proven in epoxy vitrimer formulations.[41,46–48] TBD is a well-known transesterification catalyst with a guanidine structure, including secondary, tertiary amine, and imine functions.[49] Its structure makes it a strong base, potentially initiating anionic ring-opening polymerisation (ROP)[50] of epoxides. For comparison, mixtures of the diepoxide with 2-phenyl-imidazole (2-PI), which is known as an effective anionic initiator, were also investigated. The structures of the monomers and catalysts are shown in Table 1 and the ESI Scheme S1.†
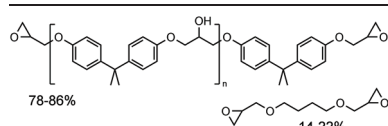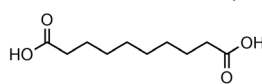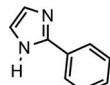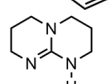
Sample preparation

The diepoxide monomer (DE) – Araldite LY564 – was purchased from Huntsman Ltd; sebacic acid (SA) 2-phenylimidazole (2-PI) and 1,5,7-triazabicyclo[4.4.0]dec-5-ene (TBD) were supplied by Tokyo Chemical Industry Ltd Belgium. Sebacic acid and TBD were added to epoxy as received and mixed for 24 h at 50 °C until a white homogeneous liquid was obtained. The final mixture was then poured into molds, to give rectangular 60 mm × 60 mm × 5 mm, and dog-bone shaped specimens measuring 115 mm × 33 mm × 6 mm, according to the ASTM standard 638 Type IV. The samples were degassed under vacuum for 2 h at 90 °C to ensure the removal of possible air bubbles formed during mixing. The samples were cured at 145 °C for 8 h (ramp 1.7 °C min^{-1} from room temperature to 145 °C), and then post-cured at 160 °C for 8 h. A schematic of sample fabrication is shown in Fig. S1.†

A series of samples was produced with different epoxy/SA ratios (summarised in Table 2). The reaction was performed using a 1 : 1 ratio of functional groups of epoxy to sebacic acid in the presence of TBD added as a 5% molar equivalent (meq.) of the epoxy group. The resulting material system was labelled 100H5CAT. Samples were prepared with different epoxy/SA ratios to explore the effect of reducing acid content in the vitrimer, as follows: 1 : 0.75, 1 : 0.6, 1 : 0.5, and 1 : 0.3, the respective materials were labelled as 75H, 60H, 50H and 30H. All reactive

Table 1 Reactants used in this study; eew: epoxy equivalent weight, mw: molecular weight, ROP: ring opening polymerisation

Chemical structure	Compound	Acronym	M (g mol^{-1})
	Diepoxide monomer (LY564)	DE	172–176 (eew)
	Diacyl monomer (sebacic acid)	SA	202.2 (mw)
	Initiator of anionic ROP (2-phenylimidazole)	2-PI	144.2 (mw)
	Transesterification catalyst (1,5,7-triazabicyclo[4.4.0]dec-5-ene)	TBD	139.2 (mw)

Table 2 Sample identification based on the epoxy/sebacic acid ratio and catalyst amount

Samples label						
	100H5CAT	75H5CAT	60H5CAT	50H5CAT	30H5CAT	30H10CAT
DE (meq.)	100	100	100	100	100	100
SA (meq.)	100	75	60	50	30	30
TBD (meq.)	5	5	5	5	5	10

mixtures in this series were prepared using 5% meq. TBD relative to the epoxy group, except the one with 10% meq. TBD, following the work of Leibler and coworkers,[31] and labelled as 5CAT and 10CAT, respectively (Table 2).

IR monitoring of the curing process

Attenuated total reflection infrared spectroscopy (ATR-IR) was performed using a Specac high-temperature Golden Gate ATR cell mounted on a Bruker Tensor 37 IR spectrometer. Curing took place at 125 °C and the IR data were collected during the first 60 minutes of the process, showing the change in the mixture composition. Samples with 5% catalyst were studied with different epoxy/acid ratio (100H, 50H and 30H). For this study, most relevant information was found in the 900–2000 cm^{-1} wavenumber range shown in Fig. S2.† Due to the overlapping of signals, monitoring was performed through the integration of absorbance over well-defined intervals. The method of analysis for ATR IR curing and integration of relevant IR signatures can be found in the ESI (Fig. S2–S5†).

Swelling and soluble fraction analysis

Swelling studies were performed using samples measuring approximately 5 mm × 5 mm × 3 mm. The samples were weighed and their dimensions measured before immersion in 1,2,4 trichlorobenzene (TCB) at 135 °C (well above the T_α of the samples), after 3 days and 1 week to ensure that swelling equilibrium has been reached. TCB was chosen for its high vaporisation temperature (214 °C). Swollen samples were extracted, wiped with a tissue, and stabilised at room temperature for 2

days to avoid any thermal expansion effect; swelling ratio and soluble fraction were calculated by gravimetry for all samples.

Mechanical test methods

Dynamic mechanical analysis (DMA) and creep experiments were performed using a Q800 DMA (TA Instruments, USA) operating in the dual cantilever mode on rectangular samples (55 mm × 15 mm × 4 mm) with a heating regime of −30 °C to 200 °C at 3 °C min^{-1}, and a measurement frequency of 1 Hz following standard procedures to measure the glass transition temperature (T_α).

Stress relaxation experiments were conducted using a Q800 DMA (TA Instruments, USA) operating in the shear mode on rectangular samples (50 mm × 50 mm × 4 mm) with 1% strain applied and allowed to relax for 500 min at each temperature level. Temperature parameters have been adapted for each sample type according to their mechanical properties.

Creep testing was performed on rectangular samples (55 mm × 15 mm × 4 mm) cut from larger plates to observe bulk relaxation. A dual cantilever clamping system was chosen to minimise the noise due to measurement. Measurements were performed at several temperatures (from 110 °C to 190 °C every 10 °C). The samples were heated and left to equilibrate at 110 °C for 10 min prior to applying a stress of 10 kPa (100H5CAT), 1 MPa (30H10CAT) or 100 kPa (others) for 30 min to reach the regime of linear time variation.[31] They were then left to relax for 10 min and heated to the next temperature level.

Quasi-static tensile tests were performed using 3 dog-bone specimens (115 mm × 33 mm × 6 mm) for each composition, using an Instron 5969 model testing machine, equipped with a 2 kN load cell, following the ASTM standard 638 Type IV. The samples were tested at 25 °C at a displacement rate of 3 mm min^{-1} to obtain the entire stress–strain response and elastic modulus.

Results

Analysis of vitrimer curing by ATR-IR

In an effort to gain better understanding of the network formation, infrared spectral analysis of sample curing was performed *via* ATR-IR. A typical IR spectrum of test sample 100H5CAT during curing is presented in Fig. 1, where the peaks of interest are highlighted. At the beginning of the experiment, two C=O stretching bands are already detected at $\bar{\nu} \approx 1705$ cm^{-1} and $\bar{\nu} \approx 1735$ cm^{-1}. The first is the conventional signal of a carboxylic acid in the molten state. The second, whose relative intensity increases with dilution (see ESI†) is due to interaction with the solvent (here, the epoxy resin plays the role of the solvent).[51] Once the reaction with epoxy starts, the absorption peak at 1705 cm^{-1} diminishes, while that at 1735 cm^{-1} increases, due to the C=O stretching signal of the ester (overlapped with the solvated COOH one). In parallel, the decay of the characteristic epoxy peak ($\bar{\nu} \approx 914$ cm^{-1}) was observed. The measurement of this signal is particularly important in samples with low acid content since it helps in understanding how the epoxide groups react with an off stoichiometric amount of acyl groups.
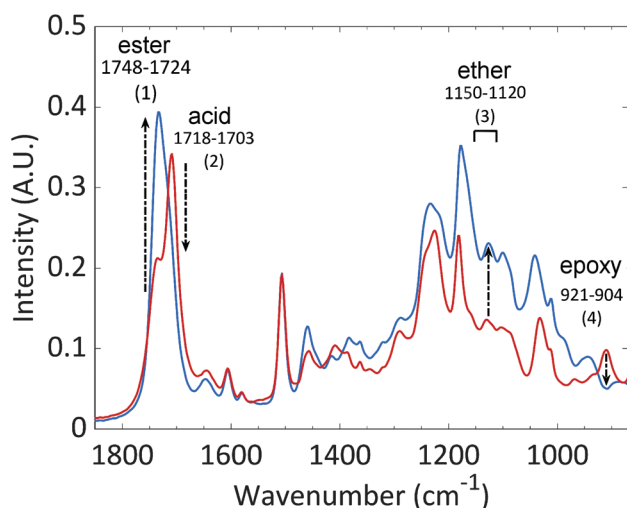

Fig. 1 ATR-FTIR spectral curve of the 100H5CAT sample at the beginning (red curve) and at the end of the reaction (blue curve). The labelled peaks correspond to: (1) C=O stretching of ester related to the polymer network, (2) C=O stretching of sebacic acid, (3) C–O–C signature of the ether, (4) asymmetric epoxy deformation. The numbers indicate signal integration intervals, see the ESI† for details of identification and integration procedure.

As for polyether formation, it is challenging to identify a single peak to characterise the homopolymerisation of epoxide due to the complexity of the infrared absorption pattern, especially when several single C–O bonds are present. However, by analysing the whole range of C–O stretching vibration ($\bar{\nu} \approx 1000$–1200 cm^{-1}) it is possible to extract a C–O–C signature and follow its relative change in different reactive mixtures (see the ESI†).

The relative change of the defined peaks over time is shown in Fig. 2 (100H5CAT and 30H5CAT). In Fig. 2a, it can be seen that acid (blue curve, triangles) and ester (red curve, squares) signals follow complementary evolutions. The acid signal shows rapid conversion to ester during the first fifteen minutes, but the reaction continues and is still not completed after 60 min of curing at 125 °C. In Fig. 2b, the signal from the epoxy (green curve, diamonds) decreases regularly throughout the first hour of curing. The ether signal (purple curve and disks) increases slowly over the time. Thus, under the conditions of 1 : 1 stoichiometry, the acid + epoxy → ester addition is predominant. Fig. 2c and d, show the evolution of the same signals for 30H5CAT. For this off-stoichiometric formulation, the acid + epoxy → ester addition reaction is clearly accelerated by an excess of epoxy; a horizontal asymptote is reached after 12–15 min. Interestingly, the etherification (Fig. 2d) does not start until the addition reaction is completed and ultimately it reaches a higher level than in the 100H5CAT compound. In parallel, the signal from the epoxy (Fig. 2d) which participates in both reactions shows a regular decrease, slower than that in 100H5CAT as expected from the law of mass action.

At 125 °C, the conversion is less than complete after 1 hour of curing. A long curing time of 8 h at 145 °C was applied to all samples to achieve optimal conversion. Analysis of epoxy residues for different stoichiometric ratios is reported in the ESI Fig. S5.† It appears that even at a low acid content (1 : 0.3), almost all epoxy groups have been consumed at the end of the reaction as shown in Fig. S5.† This suggests that even at highly unbalanced stoichiometry, residual unreacted monomers concentration remains constantly low.

In all formulations, a postcure is then necessary (*e.g.* 3000 s at 150 °C)[52] to allow equilibration of the network by transesterification reactions as reported by Altuna *et al.*[41,42] but this cannot be detected by IR spectroscopy as it does not change the nature of chemical bonds.

The question then arises whether such unbalanced systems can form a network. In our system, four main polymerisation reactions can be considered:

1. Polyaddition acid + epoxy forming a linear polyhydroxy ester (accelerated by TBD as shown in Fig. 2a).

2. Fischer esterification between free hydroxyl group and acid forming ester with the release of water (not detected in our experiments).

3. Transesterification reaction between the ester bonds and hydroxyl radicals (catalysed by TBD, not detectable by FTIR but demonstrated in the literature on small molecules).[52,53]

4. Anionic ring opening polymerisation (ROP) between epoxy groups forming ether bonds[41,42] (initiated here by TBD).

a) **100H 5CAT (TBD)**

b) **100H 5CAT (TBD)**

c) **30H 5CAT (TBD)**
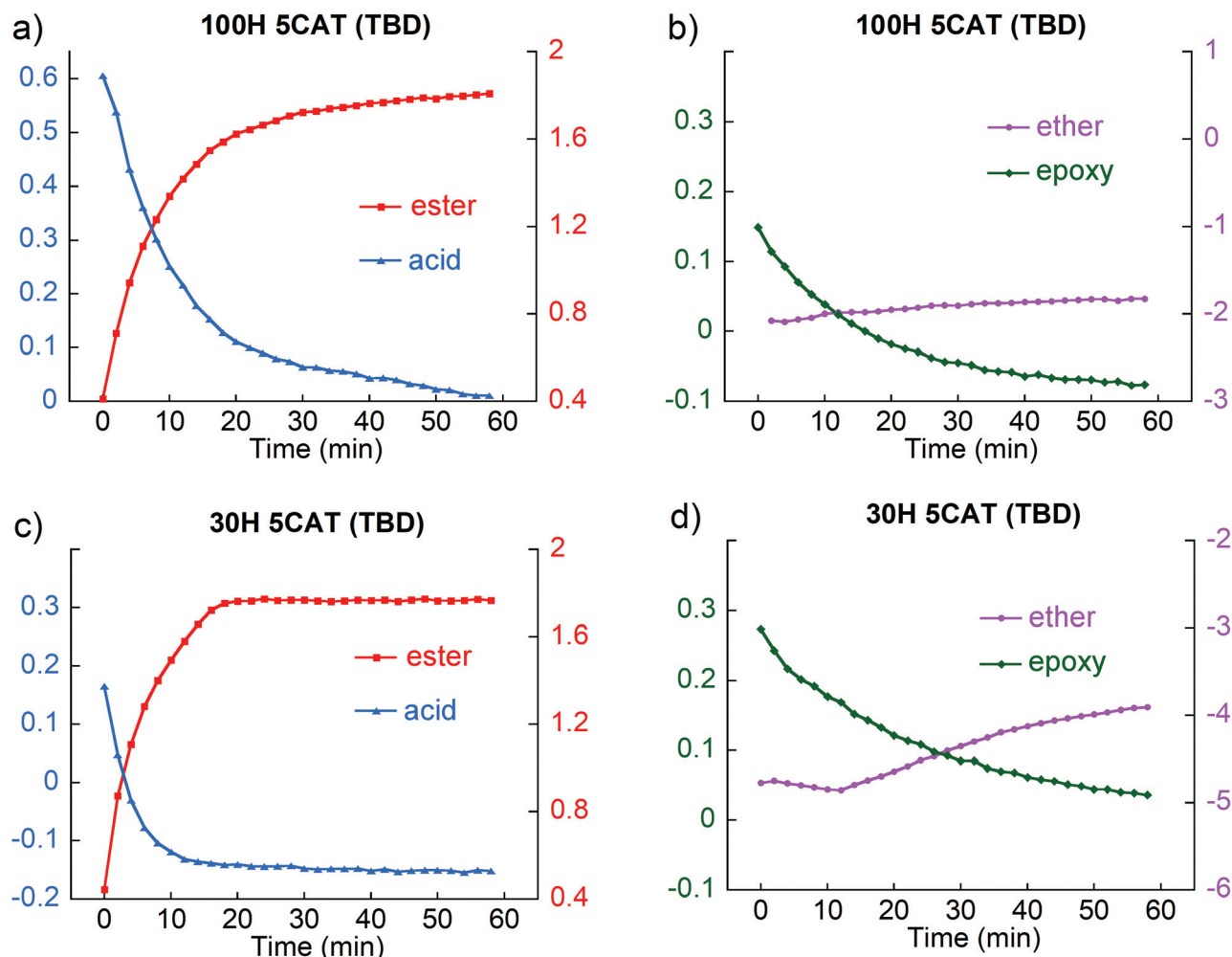
d) **30H 5CAT (TBD)**

Fig. 2 Evolution of species for different ratios of polymer network (a and b) 100H5CAT, (c and d) 30H5CAT. Measurements were performed for 60 min at 125 °C; Y-scales for each signal correspond to the values of ATR peak integrals (without normalisation, see Fig. 1 and the ESI† for details).

Regarding reaction (1) (illustrated in Scheme 1), the two monomers are bifunctional (diacid and diepoxy). This reaction essentially leads to linear products, whose molar mass is determined from the conversion and feed ratio values; virtually infinite molar masses are achievable only at exact stoichiometry. If reaction (1) (polyaddition) was the only one to occur, the gel point would not be reachable, even more, under off-stoichiometry conditions. In this case, the material properties would

be expected to range from low viscous oil to entangled thermoplastic polymer ones.

Reactions (2)–(4) are all expected to produce branching, potentially leading to a crosslinked polymer. Reaction (2) would require opposite off-stoichiometry conditions (excess of SA) and an acidic environment to take place. It is unlikely to occur with reactive mixtures catalysed by TBD (inducing a basic environment).
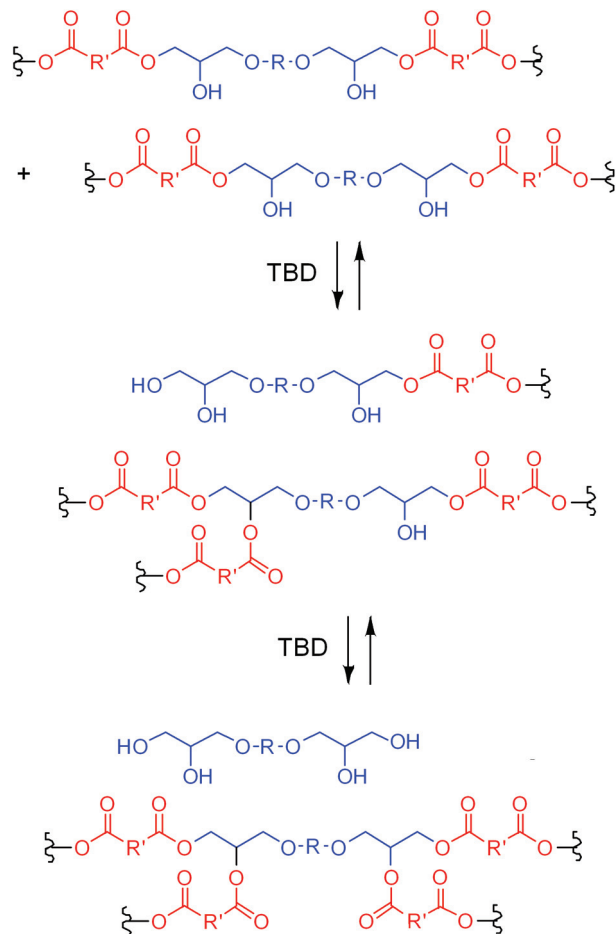
Branching by reaction (3) (transesterification), as illustrated in Scheme 2, is likely to occur in the presence of TBD but the occurrence of gelation through this process is less than obvious because each time a new branching is created by transesterification exchange, another link is broken somewhere.

Under this circumstance, the relationship between composition and the possibility of gelation may be estimated using the Flory–Stockmayer model:[54,55]
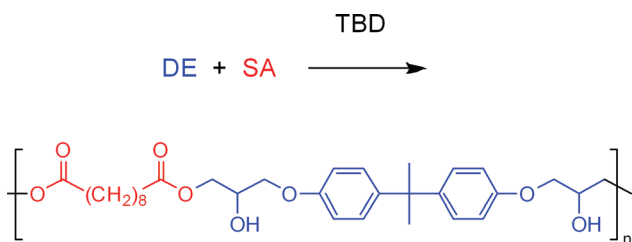
Scheme 1 Formation of exchangeable hydroxyl ester links by polyaddition of DE and SA.

$$p = \frac{1}{\sqrt{r(1 - f_A)(1 - f_B)}} \qquad (1)$$

Scheme 2 Branching by the transesterification mechanism, leading to exchangeable cross-links. The scheme illustrates the equilibrium between mono-, di-, tri-, tetraesters and the free diglycol form.

where p is the extent of reaction at the gel point, f_A and f_B the average functionality of the monomers carrying functions A and B respectively and r the stoichiometric ratio of functions A and B ($r \leq 1$). This model was developed for polycondensation, it assumes equireactivity throughout the process and the absence of loops but makes no hypothesis with regards to the chronology of forming bonds. For gelation to take place, eqn (1) must have a solution with $p < 1$.

Once transesterification is activated, the diglycol units generated by opening the diepoxide monomers can exist in the form of mono-, di- tri- and tetra-esters as well as in the free diglycol form (Scheme 2).

The diglycol unit therefore expresses a functionality $f_B = 4$, while it remains bifunctional in the absence of transesterification. When assuming equi-reactivity of all alcohol groups, transesterification of the (1:1) composition would reach the same equilibrium as condensation of one mol diacid with one mole diglycol where eqn (1) with $f_A = 2$, $f_B = 4$ and $r = 0.5$ predicts gelation.[52] For the (1:0.75) composition, $r = 0.375$, gelation is still predicted but requires a high value of conversion ($p = 0.94$). For compositions farther from stoichiometry, 1:0.6,

1:0.5, and 1:0.3 gelation would not take place if additions and transesterifications were the only reactions to occur. Gelation of polyhydroxyesters formed by 1:1 amounts of diepoxides and dicarboxylic acids has been investigated both theoretically and experimentally.[41,42,52,56,57] Further statistical study, based on the branching theory[57] also confirms the passage of the gel point in a diacid-diepoxide system able to reorganise.
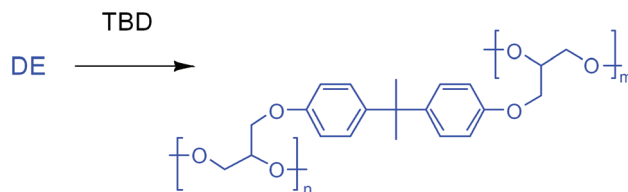
Reaction (4) (chain polymerisation by anionic ROP), illustrated in Scheme 3, is likely to occur in a basic environment and promote gelation whenever epoxy is in excess. Additional links thereby formed are not ester linkages but non-exchangeable ether links. Regarding this reaction, the diepoxide monomer is tetrafunctional and able to form crosslinks. Previous observations[41,42] demonstrate that epoxy vitrimer formulations containing 1:2 excess of epoxy and 1-methyl imidazole as an initiator form networks though this reaction.

With TBD, reaction (3) (transesterification) is known to be fast[49,52,53] and allows the gel point to be passed quickly, while reaction (2) (Fischer esterification) and reaction (4) are slow but increase the crosslink density of the 3D network. Reactions (1) and (2) terminate when there is no more acid, whereas reaction (4) continues until there is no epoxy left and slows down with a decrease in the epoxy concentration. Therefore, in all samples with TBD and excess epoxy the formation of the network is associated with reactions (1), (3) and (4).

Curing in the presence of a catalyst, which is at the same time a strong base, still raises questions whether the epoxy homopolymerisation can take place rather than the addition reaction between acid and epoxy. Hence, curing of epoxy was investigated by comparing the differences in the evolution of IR signals for 30H5CAT-type compositions containing an (100:30) excess of epoxy mixed with 5% meq. of either TBD or 2-PI. 2-PI is known to be an effective initiator of anionic ROP of epoxides.[37]

Variations in the IR signals of TBD and 2-PI based samples are plotted in Fig. 2c and d and in Fig. 3 respectively, using the same scales as Fig. 2.

With 2-PI, the ester and acid traces mirror each other (Fig. 3a) and reach complete conversion within about 8 minutes. As for the ether signal, first it shows an induction period of about 5 minutes, then a steep increase correlated with the disappearance of the COOH functions and eventually saturation after about 12 min. As for the epoxy signal, it clearly shows two different slopes for both of the above reactions, first

Scheme 3 Branching mechanism *via* anionic ROP of diepoxides–ether bonds thereby formed are not exchangeable.
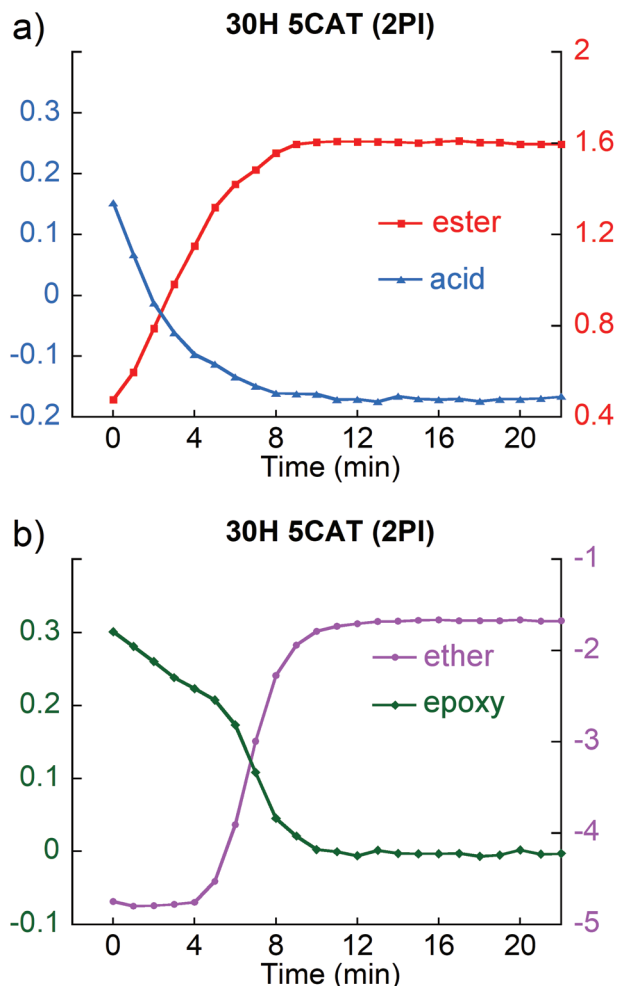
Fig. 3 Evolution of IR signals of a reactive composition containing a (100 : 30) molar excess of epoxy and 5 mol% of 2-PI as the catalyst (a) ester and acid signals, (b) ether and epoxy signals. Same *Y*-scales as Fig. 2.

and epoxy homopolymerisation propagates as long as alkoxide anions are present.

Once the acid is exhausted (after approx. 4 min for 2-PI, 12 min for TBD) the conversion of epoxy accelerates with 2-PI (Fig. 3b) while nothing similar happens with TBD (Fig. 2d). 2-PI is known to be a nucleophile, which can directly attack the epoxy through the formation of a zwitterionic adduct[59] and is regenerated after ROP propagation,[60,61] a mechanism consistent with acceleration after the consumption of the acid. In TBD, the nucleophilic imine function neighbours with a H-bonding secondary amine function. This capping property is favourable to complex alkoxide and activated acyl functions at a suitable position for transesterification,[50] but may de-activate nucleophilic species involved in the anionic ROP of epoxy.

On the other hand, TBD is significantly more basic than an imidazole (pK_a of the conjugate acid >20 for TBD[62] compared to a value of 6.48 of 2-PI[63]). TBD potentially attacks epoxy *via* the formation of oxygenated anions: alkoxide or carboxylate, rather than directly.

The fact that homopolymerisation is slower with TBD increases the probability of hydrolytic terminations *e.g.* with water molecules, conducive to the appearance of additional hydroxyl groups able to participate in the exchange reactions.

Swelling and soluble fraction analysis

The results of swelling experiments are summarised in Fig. 4. All samples swelled in TCB and remained insoluble indicating that network polymer chains are indeed in a good solvent environment and chemically bound to the rest of the network.

For 100H5CAT, the soluble fraction ≈25% is close to the predicted value.[57] The obtained network shows a decrease in its soluble fraction, concomitant with a decrease in the acyl content of the samples due to an increased crosslinking density and epoxy homopolymerisation. In contrast, the swelling ratio increases as the soluble fraction decreases with the acyl content. It is notable that the 30H10CAT sample exhibited a slightly higher swelling ratio than 30H5CAT (≈49% against ≈40%). As shown below in the DMA data, this difference correlates with a slightly lower elastic modulus of the former. This

a slow conversion stage during the reaction with the acid then a faster stage during anionic homopolymerisation.

If we compare with 2PI, the overall speed of reactions is slower than with TBD, the two reactions are more clearly decoupled with 2PI but in both cases, the scenario is the same: a first wave is observed, corresponding to the addition reactions (Fig. 2a and b) then a second wave due to anionic homopolymerisation. The proposed mechanism is very similar to that depicted in Schemes 1 and 2 in ref. 58 for a thiol–epoxy system. The base (either TBD or 2-PI) deprotonates the COOH function, producing a carboxylate anion which can attack the epoxy group and produce an alkoxide anion. In the presence of excess acid groups, a rapid proton exchange between the alkoxide anion and the acid takes place (because of the difference in pK_a of the alcohol/alkoxide and acid/carboxylate pairs) leading to the formation of another carboxylate anion and a hydroxyester group. In off-stoichiometric formulations, once the acid is depleted this proton transfer does not take place
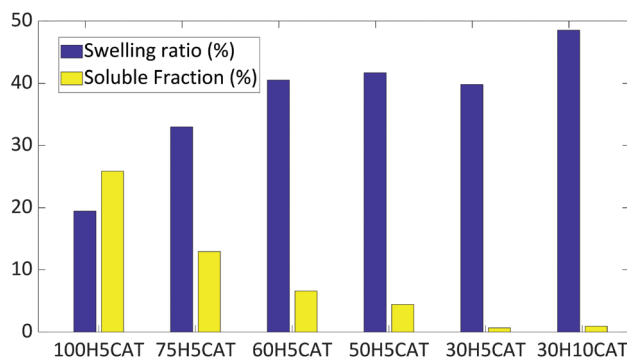

Fig. 4 Swelling experiment to confirm the crosslinking of the structure, mass increase (blue) and mass fraction of the soluble part (yellow).

indicates a higher crosslink density upon decreasing the amount of initiator for these off-stoichiometric compositions, where formation of the network is dominated by chainwise polymerisation. Overall, none of these samples were dissolved and are considered to have crosslinked beyond the gel point.

Mechanical properties at small and large deformations

DMA results, summarised in Fig. 5, show that when the acid content of the prepared vitrimers decreases (from 1 : 1 meq. to 1 : 0.3 meq. epoxy : acid), the glass transition temperature (tan delta peak values, Table S1†) gradually increases, from ~40 °C (sample 100H) to ~100 °C (samples 30H). This variation follows the rule of mixtures described by the Fox–Flory equation, as also observed in the off-stoichiometry thiol-epoxy formulation,[64,65] thus demonstrating the homogeneity of the networks (Fig. S6†). The catalyst loading (5% or 10% meq. of epoxy) did not change the T_α of the 30H sample type but rubbery plateau modulus was lower with a higher catalyst content. To summarise, it appears that the T_α and the rubbery plateau can be tuned by changing the stoichiometric ratio between the epoxy and hardener. It is worth noting that in our system the term "soft crosslinker" would be more appropriate than hardener.

The maximum of the loss tangent peak (Fig. 5b) gradually decreases concomitantly with the sebacic acid content. This observation should be correlated with the evolution of a soluble fraction in the same series. Higher damping ability is related to the amount of network defects (*i.e.* dangling chains, isolated microgel fragments, and oligomers). The presence of such defects in samples close to stoichiometry proves a crosslinking mechanism mostly related to exchanges by transesterification as illustrated in Scheme 3. Whereas, off-stoichiometric compounds appear to be more tightly crosslinked, due to crosslinking mechanism by anionic ROP as illustrated in Scheme 2.

Tensile tests were conducted and representative stress/strain curves for different stoichiometric ratios investigated are presented in Fig. 6. Sample 100H5CAT exhibited significant elongation (>300%) and low stress at break (<2 MPa), and Young's modulus (0.5 MPa) corresponding to a lightly crosslinked elastomer. Once the content of acid is decreased (75H5CAT sample), the tensile response shows an increase of initial Young's modulus (1.6 MPa) and strength (>10 MPa), and concomitant decrease in the strain at break (~140%). At lower acid contents (50H5CAT and 30H5CAT), the materials behave like a stiff epoxy thermoset with Young's modulus in the GPa range, and strength around 50 MPa.

100H5CAT behaves like a low-density crosslinked elastomer due to the length and size of the SA fragment and its relatively low T_α (~40 °C). When the acid content is reduced, the homopolymerisation of epoxy leads to lower average distance between hard fragments of the epoxy backbone closely con-
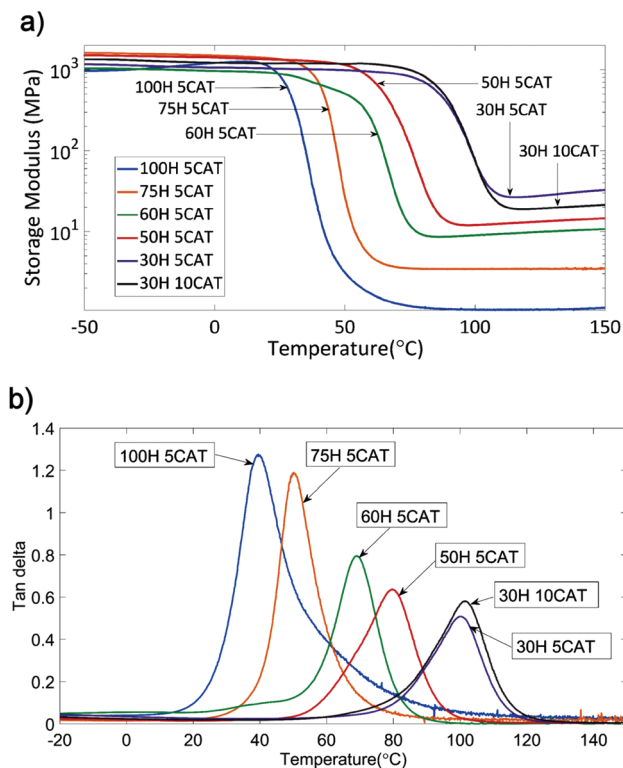

Fig. 5 (a) Storage moduli for different ratios, obtained by DMA measurements; (b) damping response of tested samples.
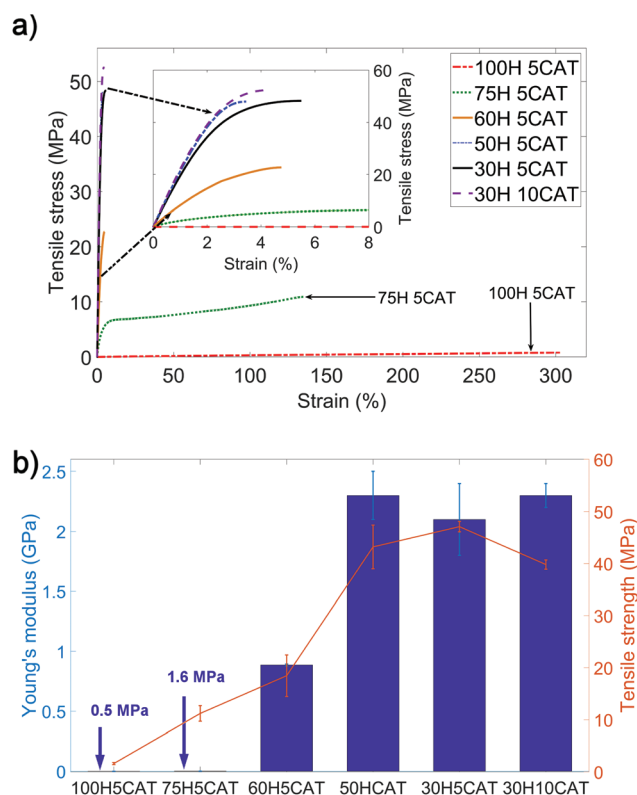

Fig. 6 Tensile behaviour obtained with ASTDM 638 type IV samples. (a) Typical stress/strain curves obtained for each epoxy : acid ratio, (b) bar chart and curve comparing Young's moduli and tensile strengths of the samples.

nected by glycerol units (Scheme 2). In contrast to SA/epoxy bonding that regularly introduced a flexible spacer between them (Schemes 1 and 3).

Performance of off-stoichiometric samples are very similar to conventional epoxies used in industries, with sebacic acid being a relatively cheap and safe "hardener" to handle. Mechanical data are summarised in Table S2.†

Stress relaxation of epoxy vitrimers

The capacity of relaxing stress was measured to ascertain the impact of off-stoichiometric formulation. The difference in mechanical properties required adapting the testing temperature for each sample examined (the stronger the network is, the higher the temperature must be). Sample type 100H5CAT and 75H5CAT exhibit complete stress relaxation as shown in Fig. 7a and Fig. S7b.† For 60H5CAT, at 180 °C, the stress hardly relaxes down to 10% of the initial value after 20 000 s (Fig. 7b) and application of higher temperature caused observable chemical degradation of the network and significant deviation from exponential decay at this time scale (Fig. S7c†). Similar behaviour is observed for the 50H5CAT sample with stress relaxed down to 20% of the initial value (Fig. S7d†). 30H samples (5CAT and 10CAT) both exhibit a tendency to relax down to a value of $G/G_0 \approx 0.2$ (Fig. 7c). These results are in line with the findings of Torkelson and coworkers,[44] where vitrimers with <50% of unexchangeable covalent bonds were found to exhibit a near full relaxation. When the network is composed of more than 50% of irreversible bonds, it is only able to relax about 70% of the applied strain (30H5CAT and 10CAT samples correspond to 70% irreversible covalent bond content in the network).

Creep behaviour of epoxy vitrimers

The flow properties of the materials were also evaluated using creep experiments. As pointed out recently, this method is useful for characterizing vitrimers with very slow dynamics,[66] and avoids the shortcoming of low force measurements. Creep data of the same three samples under an applied stress of 0.1 MPa (75H5CAT and 60H5CAT), and 1 MPa (30H10CAT) are presented in Fig. 8. Evidently, the sample closest to stoichiometry (75H5CAT, Fig. 8a) flows like a liquid with the deformation increasing linearly with time, as also observed for the 100H5CAT sample (Fig. S8b†). Moving further towards off-stoichiometry samples (60H5CAT), creep data do not exhibit a capacity to flow as the acquired deformation after 30 min is still well below 1% and the overall variation is not linear with time. This demonstrates that despite its capacity to nearly relax full stress under 1% applied deformation, 60H5CAT is, however, unable to flow like a liquid. Such observations lead to the conclusion that this material cannot be recognised as a vitrimer, but rather as a vitrimer-like material as defined in ref. 67 and 68, showing the ability to be welded or healed but not entirely reshaped. Moving further to using an acyl content of 50% and lower (50H5CAT, 30H5CAT and 30H10CAT), any ability to flow disappears from creep profiles (Fig. S8d, e† and
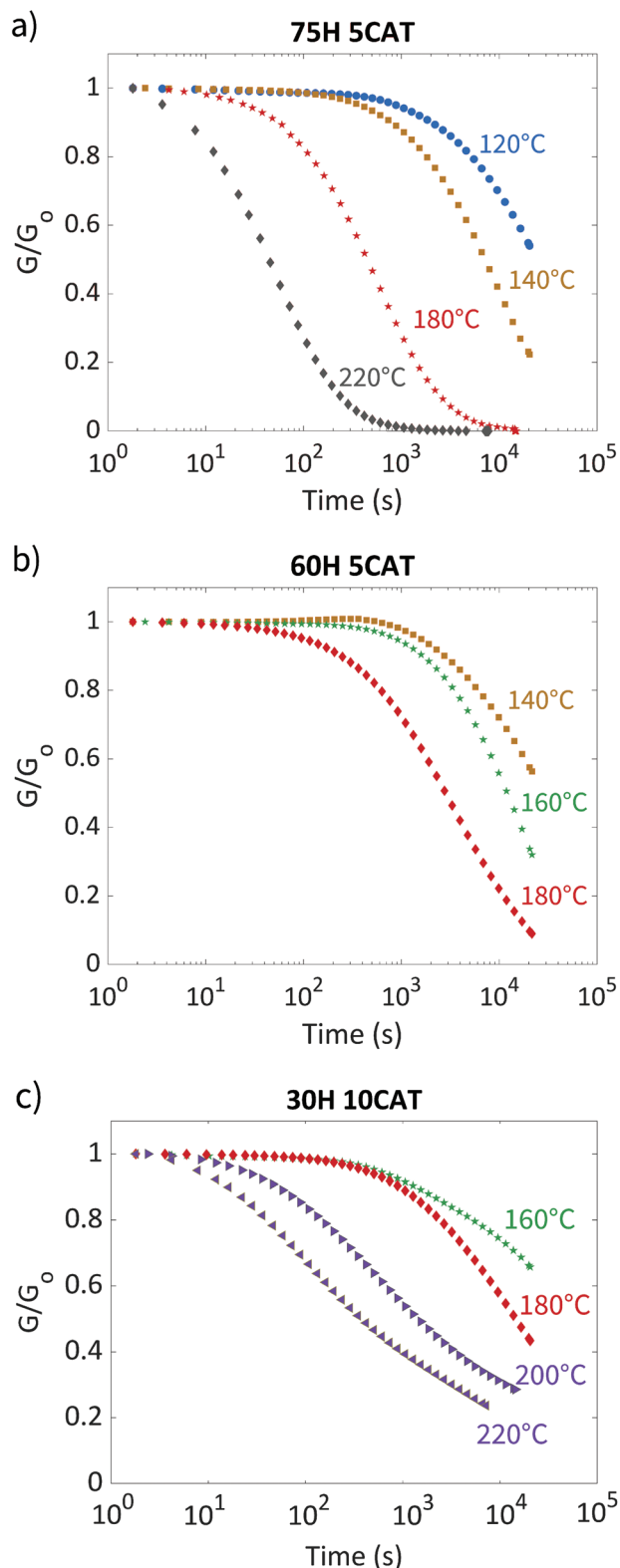

Fig. 7 Stress relaxation at different temperatures for three different epoxy/acid ratios: (a) 75H5CAT, (b) 60H5CAT, and (c) 30H10CAT.
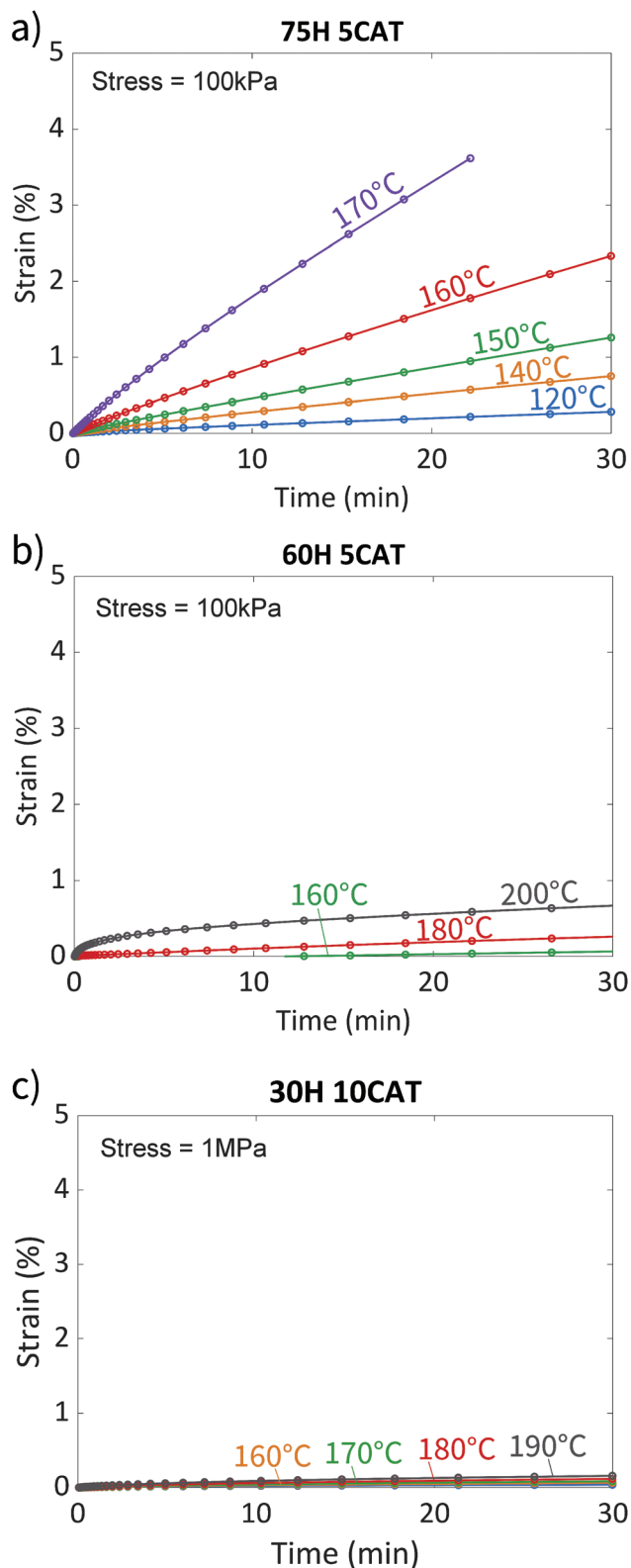
Fig. 8   Creep behaviour for different temperatures and three different epoxy/acid ratios: (a) 75H5CAT, (b) 60H5CAT, and (c) 30H10CAT.

Fig. 8c) and the data rather suggest shape fixity of an essentially permanent network.

Fitting stress relaxation data of 100H5CAT by a single exponential decay allows one to determine the relaxation time, *e.g.* at 180 °C: $\tau \sim 90$ s. The value of τ at any temperature deduced from stress relaxation data is represented as Arrhenius plot in Fig. 9a. The slope gives an activation energy of about 100 kJ mol^{-1}.

The same treatment on 75H5CAT stress relaxation data affords significantly longer relaxation times *e.g.* $\tau \sim 700$ s at 180 °C and a similar activation energy. In addition, experimental data do not completely overlap the fit, suggesting that more than one relaxation time had to be considered.
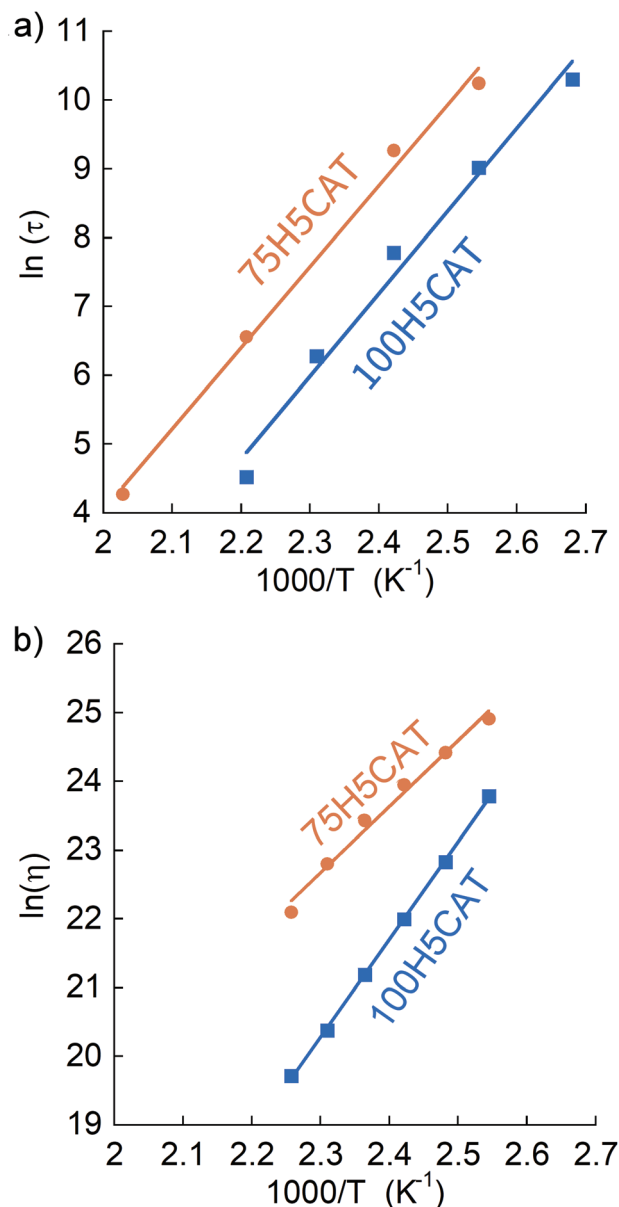

Fig. 9   Arrhenius plot from (a) stress relaxation and (b) creep data of vitrimers with two different epoxy/acid ratios.

In Fig. 9b the Arrhenius plots of the same samples are calculated from the creep data.

In this figure, the activation energy for 75h5CAT is lower and viscosity higher than that of the stoichiometric one. This indicate that the presence of sequences comprising a large number of non-exchangeable bonds induce slower relaxation modes which is not detectable by a monoexponential fit and decrease the themoresponsivity of the system.

In other samples 50H5CAT, 30H5CAT (Fig. S7d and e†), 60H5CAT, and 30H10CAT (Fig. 7b and c), the extent of stress relaxation progressively decreases concomitantly with acid content and fitting by a single exponential model can no longer be achieved.

Conclusions

The present work demonstrates that full conversion of epoxy functions is achieved despite using a relatively low acyl content compared to the epoxy amount (down to 30% of the epoxy functions). The side reactions involved in the curing of non-stoichiometric systems are not necessarily detrimental to properties of materials. Effectively, TBD promotes anionic ROP in off-stoichiometric samples, leading to branching and crosslinking of the network. However, this reaction remains slow compared to the polyaddition of epoxy and acyl functions and promotes the formation of non-exchangeable polyether chains. At any stoichiometry, the epoxy acyl curing in the presence of TBD produces an insoluble crosslinked polymer (>75% of insoluble fraction). The samples closer to stoichiometry present more defects compared to the samples with a strong off-stoichiometry composition, which explains the improvement of thermomechanical properties in the elastomeric range. The rubbery plateau and mechanical strength of the materials both increase, when departing from stoichiometry and a transition from elastomeric to glassy behaviour is observed. This transition of the thermomechanical properties with the hardener content leads to the conclusion that sebacic acid acts more as a "soft crosslinker" for this network. When decreasing the acyl content of the formulation, the network undergoes a progressive transition from a vitrimer material (100H5CAT and 75H5CAT), to a vitrimer-like[67,68] material (60H5CAT), and finally, to a permanently crosslinked material. The present study shows the potential to produce a tunable vitrimer formulation, without changing any of the manufacturing process parameters other than stoichiometry. This tuning aspect could raise practical interests for applications requiring tailored thermomechanical properties, without the need of altering the chemical formulation or handling processes.

Conflicts of interest

There are no conflicts to declare.

References

1 L. Leibler, M. Rubinstein and R. H. Colby, *J. Phys. II*, 1993, **3**, 1581–1590.

2 R. D. Andrew, A. V. Tobolsky and E. E. Hanson, *Rubber Chem. Technol.*, 1946, **4**, 1099–1112.

3 C. N. Bowman and C. J. Kloxin, *Angew. Chem., Int. Ed.*, 2012, **51**, 4272–4274.

4 C. J. Kloxin and C. N. Bowman, *Chem. Soc. Rev.*, 2013, **42**, 7161–7173.

5 X. Chen, M. A. Dam, K. Ono, A. Mal, H. Shen, S. R. Nutt, K. Sheran and F. Wudl, *Science*, 2002, **295**, 1698.

6 V. Froidevaux, M. Borne, E. Laborbe, R. Auvergne, A. Gandini and B. Boutevin, *RSC Adv.*, 2015, **5**, 37742–37754.

7 A. Gandini, *Prog. Polym. Sci.*, 2013, **38**, 1–29.

8 T. F. Scott, A. D. Schneider, W. D. Cook and C. N. Bowman, *Science*, 2005, **308**, 1615.

9 D. Montarnal, M. Capelot, F. Tounilhac and L. Leibler, *Science*, 2011, **334**, 965–968.

10 M. Capelot, D. Montarnal, F. Tournilhac and L. Leibler, *J. Am. Chem. Soc.*, 2012, **134**, 7664–7667.

11 R. L. Snyder, D. J. Fortman, G. X. De Hoe, M. A. Hillmyer and W. R. Dichtel, *Macromolecules*, 2018, **51**, 389–397.

12 Y. Spiesschaert, M. Guerre, L. Imbernon, J. M. Winne and F. Du Prez, *Polymer*, 2019, **172**, 239–246.

13 I. Azcune and I. Odriozola, *Eur. Polym. J.*, 2016, **84**, 147–160.

14 L. Zhang and S. J. Rowan, *Macromolecules*, 2017, **50**, 5051–5060.

15 S. Zhang, L. Pan, L. Xia, Y. Sun and X. Liu, *React. Funct. Polym.*, 2017, **121**, 8–14.

16 B. Hendriks, J. Waelkens, J. M. Winne and F. E. Du Prez, *ACS Macro Lett.*, 2017, **6**, 930–934.

17 M. M. Obadia, A. Jourdain, P. Cassagnau, D. Montarnal and E. Drockenmuller, *Adv. Funct. Mater.*, 2017, **27**, 1703258.

18 A. Demongeot, R. Groote, H. Goossens, T. Hoeks, F. Tournilhac and L. Leibler, *Macromolecules*, 2017, **50**, 6117–6127.

19 J. Tang, L. Wan, Y. Zhou, H. Pan and F. Huang, *J. Mater. Chem. A*, 2017, **5**, 21169–21177.

20 T. Stukenbroeker, W. Wang, J. M. Winne, F. E. Du Prez, R. Nicolaÿ and L. Leibler, *Polym. Chem.*, 2017, **8**, 6590–6593.

21 A. Arnebold, S. Wellmann and A. Hartwig, *Polymer*, 2016, **91**, 14–23.

22 A. Arnebold, S. Wellmann and A. Hartwig, *J. Appl. Polym. Sci.*, 2016, **133**, 43986.

23 V. R. Sastri and G. C. Tesoro, *J. Appl. Polym. Sci.*, 1990, **39**, 1439–1457.

24 J.-P. Pascault and R. J. J. Williams, *Epoxy Polymers: New Materials and innovations*, Wiley, 2010.

25 M. Holst, K. Schänzlin, M. Wenzel, J. Xu, D. Lellinger and I. Alig, *J. Polym. Sci., Part B: Polym. Phys.*, 2005, **43**, 2314–2325.

26 X. Fernàndez-Francos, S. G. Kazarian, X. Ramis and À. Serra, *Appl. Spectrosc.*, 2013, **67**, 1427–1436.

27 J. Scheirs and T. E. Long, *Modern Polyesters: Chemistry and Technology of Polyesters and Copolyesters; Chap II and V*, John Wiley and Sons Ltd., Chichester, 2003.

28 M. Delahaye, J. M. Winne and F. E. Du Prez, *J. Am. Chem. Soc.*, 2019, **141**, 15277–15287.

29 F. Ma and M. A. Hanna, *Bioresour. Technol.*, 1999, **70**, 1–15.

30 W. Liu, D. F. Schmidt and E. Reynaud, *Ind. Eng. Chem. Res.*, 2017, **56**, 2667–2672.

31 M. Capelot, M. M. Unterlass, F. Tournilhac and L. Leibler, *ACS Macro Lett.*, 2012, **1**, 789–792.

32 A. S. Hoffman, *Adv. Drug Delivery Rev.*, 2013, **65**, 10–16.

33 J. Otera, *Chem. Rev.*, 1993, **93**, 1449–1470.

34 A. Demongeot, S. J. Mougnier, S. Okada, C. Soulié-Ziakovic and F. Tournilhac, *Polym. Chem.*, 2016, **7**, 4486–4493.

35 E. Chabert, J. Vial, J.-P. Cauchois, M. Mihaluta and F. Tournilhac, *Soft Matter*, 2016, **12**, 4838–4845.

36 A. Ruiz de Luzuriaga, R. Martin, N. Markaide, A. Rekondo, G. Cabañero, J. Rodríguez and I. Odriozola, *Mater. Horiz.*, 2016, **3**, 241–247.

37 V. Rebizant, A.-S. Venet, F. Tournilhac, E. Girard-Reydet, C. Navarro, J.-P. Pascault and L. Leibler, *Macromolecules*, 2004, **37**, 8017–8027.

38 Q. Shi, K. Yu, X. Kuang, X. Mu, C. K. Dunn, M. L. Dunn, T. Wang and H. Jerry Qi, *Mater. Horiz.*, 2017, **4**, 598–607.

39 Y. Yang, Z. Pei, X. Zhang, L. Tao, Y. Wei and Y. Ji, *Chem. Sci.*, 2014, **5**, 3486–3492.

40 K. Yu, P. Taynton, W. Zhang, M. L. Dunn and H. J. Qi, *RSC Adv.*, 2014, **4**, 48682–48690.

41 F. I. Altuna, C. E. Hoppe and R. J. J. Williams, *RSC Adv.*, 2016, **6**, 88647–88655.

42 F. Altuna, C. Hoppe and R. Williams, *Polymers*, 2018, **10**, 43.

43 L. Matějka, S. Pokomý and K. Dušek, *Polym. Bull.*, 1982, **7**, 123–128.

44 L. Li, X. Chen, K. Jin and J. M. Torkelson, *Macromolecules*, 2018, **51**, 5537–5546.

45 C. E. Hoppe, M. J. Galante, P. A. Oyanguren and R. J. J. Williams, *Macromol. Mater. Eng.*, 2005, **290**, 456–462.

46 F. I. Altuna, C. E. Hoppe and R. J. J. Williams, *Eur. Polym. J.*, 2019, **113**, 297–304.

47 Z. Pei, Y. Yang, Q. Chen, E. M. Terentjev, Y. Wei and Y. Ji, *Nat. Mater.*, 2014, **13**, 36–41.

48 Z. Pei, Y. Yang, Q. Chen, Y. Wei and Y. Ji, *Adv. Mater.*, 2016, **28**, 156–160.

49 B. G. G. Lohmeijer, R. C. Pratt, F. Leibfarth, J. W. Logan, D. A. Long, A. P. Dove, F. Nederberg, J. Choi, C. Wade, R. M. Waymouth and J. L. Hedrick, *Macromolecules*, 2006, **39**, 8574–8583.

50 R. C. Pratt, B. G. G. Lohmeijer, D. A. Long, R. M. Waymouth and J. L. Hedrick, *J. Am. Chem. Soc.*, 2006, **128**, 4556–4557.

51 E. Cazares-Cortes, B. C. Baker, K. Nishimori, M. Ouchi and F. Tournilhac, *Macromolecules*, 2019, **52**, 5995–6004.

52 M. Capelot, *Chimie de Polycondensation, Polymères Supramoléculaires et Vitrimères*, Université Pierre et Marie Curie, Paris VI, 2013.

53 U. Schuchardt, R. Sercheli and R. M. Vargas, *J. Braz. Chem. Soc.*, 1998, **9**, 199–210.

54 P. J. Flory, *J. Am. Chem. Soc.*, 1941, **63**, 3083–3090.

55 W. H. Stockmayer, *J. Chem. Phys.*, 1944, **12**, 125–131.

56 J. E. Klee, F. Claußen and H. H. Hörhold, *Polym. Bull.*, 1995, **35**, 79–85.

57 K. Dusek and L. Matejka, in *Rubber-Modified Thermoset Resins*, American Chemical Society, 1984, vol. 208, ch. 2, pp. 15–26.

58 X. Fernández-Francos, A.-O. Konuray, A. Belmonte, S. De la Flor, À. Serra and X. Ramis, *Polym. Chem.*, 2016, **7**, 2280–2290.

59 M. S. Heise and G. C. Martin, *Macromolecules*, 1989, **22**, 99–104.

60 X. Fernàndez-Francos, *Eur. Polym. J.*, 2014, **55**, 35–47.

61 S. K. Ooi, W. D. Cook, G. P. Simon and C. H. Such, *Polymer*, 2000, **41**, 3639–3649.

62 I. Kaljurand, A. Kütt, L. Soováli, T. Rodima, V. Mäemets, I. Leito and I. A. Koppel, *J. Org. Chem.*, 2005, **70**, 1019–1028.

63 H. Walba and R. W. Isensee, *J. Org. Chem.*, 1961, **26**, 2789–2791.

64 T. G. Fox and P. J. Flory, *J. Appl. Phys.*, 1950, **21**, 581–591.

65 A. Belmonte, C. Russo, V. Ambrogi, X. Fernández-Francos and S. De la Flor, *Polymers*, 2017, **9**, 113.

66 R. G. Ricarte, F. Tournilhac, M. Cloître and L. Leibler, *Macromolecules*, 2020, **53**, 1852–1866.

67 L. Imbernon, S. Norvez and L. Leibler, *Macromolecules*, 2016, **49**, 2172–2178.

68 S. Kaiser, S. Wurzer, G. Pilz, W. Kern and S. Schlögl, *Soft Matter*, 2019, **15**, 6062–6072.